Two-frequency Ramsey interferometry

D. Seidel* and J. G. Muga†
Departmento de Química-Física, Universidad del País Vasco, Apartado Postal 644, 48080 Bilbao, Spain
(Received 8 June 2006; published 16 February 2007)

We investigate Ramsey interferometry for two separated fields oscillating with different frequencies. It is shown that the interplay between average and relative detuning leads to interference effects not present in the standard, single-frequency setup. For a large free-flight time of ground-state atoms before entering the first field region, the Ramsey fringes with respect to the relative detuning become much narrower than the usual ones. The stability of these effects with respect to phase or velocity fluctuations is discussed.

DOI: 10.1103/PhysRevA.75.023811 PACS number(s): 42.50.Ct, 03.75.−b, 39.20.+q

I. INTRODUCTION

Ramsey's method of atom interferometry with separated oscillating fields [1] provides the basis of present primary time standards, like cesium-beam or cesium-fountain clocks [2]. Basically, one aims to lock an oscillator exactly at a given atomic transition frequency to achieve stability and accuracy of the oscillator and thus of the clock. The physical quantity that indicates possible deviations from the reference transition as a function of detuning is the excitation probability of the ground-state atom after the interaction with two separated oscillating fields, and this function shows the well-known Ramsey fringes. Note that as long as quantum reflections of the atom at the fields and recoil effects can be neglected, the operation of the interferometer in the time domain (temporally separated pulses and fixed atom) or in the space domain (spatially separated fields and moving atom) is equivalent for atoms moving along classical trajectories, and we shall concentrate on moving atoms hereafter.

A central requirement for frequency standards is a narrow interference pattern with respect to detuning, to allow for a precise lock of the oscillating fields to the atomic clock transition. It has been shown by Ramsey [1] that the width of the central peak of the pattern is inversely proportional to the intermediate time between the two fields T, in contrast to the single-field (Rabi) scheme, where it is inversely proportional to the field-crossing time. In cesium-beam standards, for example, this motivates the use of tall "fountain" configurations, limited in practice because of space constraints [3], or very slow (ultracold) atoms in reduced gravity [4]. Even though the dependence on the free-flight time is better than on field-crossing time because of the difficulty of implementing a homogeneous and stable field,[1] the intermediate free flight between the two fields occurs for atomic states with an excited component, which should be as stable as possible against radiative decay [5].

In this paper we investigate the use of two separated fields with *different* detuning. In this case, the interference pattern in the excitation probability will depend, in addition to the intermediate free-flight time, on the flight time of the ground-state atom before entering the fields. Within a semiclassical picture, i.e., neglecting quantum reflections at the fields, a general expression for the excitation probability as a function of average detuning and relative detuning is derived and discussed. It is shown that the interference pattern as a function of the relative detuning becomes considerably narrower than the usual Ramsey pattern if the initial phase difference of the fields is controlled. We have also examined the effect of averaging over phase or entrance-time distributions.

For simplicity of the presentation, we neglect in our calculations the transverse momentum transfer on the atom, which is reasonable for moving atoms and microwave frequencies or for trapped ions in the Lamb-Dicke regime and optical fields [6,7]. For a detailed study of these recoil effects in connection with Ramsey interferometry we refer to [8]. For freely moving atoms interacting with optical fields, one is led normally to consider the multibeam schemes proposed by Kasevich and Chu or by Bordé to compensate for the wave-packet separation due to recoil effects; see [9] for reviews. Transverse momentum transfer with optical fields could also be suppressed by confining the moving atoms in a narrow waveguide [10].[2]

II. HAMILTONIAN AND INTERACTION PICTURES

We consider the basic Ramsey setup where a two-level atom initially in the ground state moves along the x axis and crosses two separated oscillating fields localized between 0 and l and between $l+L$ and $2l+L$ (Fig. 1).

In contrast to the standard setting, we allow for different detuning of the two fields with respect to the atomic transition frequency ω_{21}. The measured quantity is the transmission probability of excited atoms, P_{12}, as a function of the

*Electronic address: dirk_seidel@ehu.es
†Electronic address: jg.muga@ehu.es

[1]For trapped ions, though, the single-pulse Rabi scheme may be preferred to the Ramsey scheme; see, e.g., [15].

[2]For a waveguide width of 100 nm and for cesium, the energy gap to the first transversely excited state is $\delta E = 2\pi\hbar \times 0.113$ MHz. Now, a minor modification of Ref. [11] to incorporate detuning shows that excitation mainly occurs at the "Rabi resonances" $\hbar(\Omega^2+\Delta^2)^{1/2} = \delta E$, where Ω is the Rabi frequency and $\Delta = \omega - \omega_{21}$ denotes the detuning between laser frequency and atomic transition frequency. For Rabi frequencies of the order of $2\pi \times 0.016$ MHz one therefore would have a detuning range $\Delta \approx 2\pi \times (-0.11 - 0.11)$ MHz for which transversal excitation can be neglected.

detuning $\Delta_j=\omega_j-\omega_{21}$, $j=1,2$, where ω_j is the frequency of the jth field. The Hamiltonian describing the moving atom and the field reads in the dipole and rotating-wave approximation and in the Schrödinger picture

$$H(t)=\frac{\hat{p}^2}{2m}+\hbar\omega_{21}|2\rangle\langle 2|+\sum_{j=1,2}\frac{\hbar\Omega_j(\hat{x})}{2}(|1\rangle\langle 2|e^{i\omega_j t+i\phi_j}+|2\rangle \times\langle 1|e^{-i\omega_j t-i\phi_j}), \tag{1}$$

where $\Omega_j(x)$, $j=1,2$, are the Rabi frequencies of the two spatially localized fields, ϕ_1 and ϕ_2 are their phases at $t=0$, and the caret is used to distinguish operators from the corresponding c numbers. Note that for $\omega_1\neq\omega_2$ there is no interaction picture for which this time-dependent Hamiltonian can be made time-independent, as it is the case for $\omega_1=\omega_2$.

In the atom-adapted interaction picture with $H_0=\hbar\omega_{21}|2\rangle\langle 2|$ one has

$$H_{\rm I}(t)=\frac{\hat{p}^2}{2m}+\sum_{j=1,2}\frac{\hbar\Omega_j(\hat{x})}{2}(|1\rangle\langle 2|e^{i\Delta_j t+i\phi_j}+|2\rangle\langle 1|e^{-i\Delta_j t-i\phi_j}). \tag{2}$$

In this interaction picture, the atom-field interaction is zero between the fields and therefore we will favor it for the calculation of P_{12}.

III. SEMICLASSICAL SOLUTION OF THE SCHRÖDINGER EQUATION

For fast enough particles, i.e., for kinetic energies $E=mv^2/2=\hbar^2k^2/2m$ much larger than $\hbar\Omega$ and $\hbar\Delta_j$, the center-of-mass motion of the atom can be treated classically and independently of the internal dynamics [12]. Within that approximation, the two-component wave function $|\psi_{\rm I}(t)\rangle$ which accounts for the internal dynamics in the interaction picture is a solution of the internal Schrödinger equation

$$i\hbar\frac{d}{dt}|\psi_{\rm I}(t)\rangle=H_{\rm I}^{\rm scl}(t)|\psi_{\rm I}(t)\rangle, \tag{3}$$

where

$$H_{\rm I}^{\rm scl}=\sum_{j=1,2}\frac{\hbar\Omega(x_0+vt)}{2}(|1\rangle\langle 2|e^{i\Delta_j t+i\phi_j}+|2\rangle\langle 1|e^{-i\Delta_j t-i\phi_j}) \tag{4}$$

and $x_0<0$ is the position of the atom at time $t=0$. In the following, we consider the internal dynamics for a given kinetic energy E, i.e., for a single atom whose center of mass follows the classical trajectory $x(t)=x_0+vt$. We denote by t_0 the time of the first interaction with the leftmost field, $t_0=-x_0/v$. This treatment neglects initial uncertainties in position and momentum. The general case with an initial position and momentum distribution leads to a distribution of entrance times t_0 and it is considered later in Sec. VI.

The solution of Eq. (3) is given in terms of the evolution operator $U_{\rm I}(t_f,t_i)$,

$$|\psi_{\rm I}(t_f)\rangle=U_{\rm I}(t_f,t_i)|\psi_{\rm I}(t_i)\rangle, \tag{5}$$

where $U_{\rm I}(t_f,t_i)$ satisfies

$$i\hbar\frac{d}{dt}U_{\rm I}(t_f,t_i)=H_{\rm I}^{\rm scl}(t_f)U_{\rm I}(t_f,t_i),$$

$$U_{\rm I}(t_i,t_i)=U(t_i,t_i)=\hat{1}. \tag{6}$$

To obtain analytical results, we consider mesa mode functions for the two fields, $\Omega_1(x)=\Omega$ for $0\leqslant x\leqslant l$ and zero elsewhere and $\Omega_2(x)=\Omega$ for $l+L\leqslant x\leqslant 2l+L$ and zero elsewhere. However, by a numerical integration of Eq. (6) we have shown the stability of the results with respect to more realistic, smooth field shapes.

In the field-free regions the Hamiltonian in the interaction picture is zero and thus the evolution operator is unity. Within the jth field, the solution of Eq. (6) is given by

$$U_{\rm I}^{(j)}(t_f,t_i)=\begin{pmatrix} e^{i\Delta_j(t_f-t_i)/2}\left\{\cos\left[\frac{\Omega_j'(t_f-t_i)}{2}\right]-\frac{i\Delta_j}{\Omega_j'}\sin\left[\frac{\Omega_j'(t_f-t_i)}{2}\right]\right\} & -\frac{i\Omega}{\Omega_j'}e^{i\Delta_j(t_f+t_i)/2}e^{i\phi_j}\sin\left[\frac{\Omega_j'(t_f-t_i)}{2}\right] \\ -\frac{i\Omega}{\Omega_j'}e^{-i\Delta_j(t_f+t_i)/2}e^{-i\phi_j}\sin\left[\frac{\Omega_j'(t_f-t_i)}{2}\right] & e^{-i\Delta_j(t_f-t_i)/2}\left\{\cos\left[\frac{\Omega_j'(t_f-t_i)}{2}\right]+\frac{i\Delta_j}{\Omega_j'}\sin\left[\frac{\Omega_j'(t_f-t_i)}{2}\right]\right\}\end{pmatrix}, \tag{7}$$

where the effective Rabi frequencies $\Omega_j'=(\Omega^2+\Delta_j^2)^{1/2}$, $j=1,2$, have been defined, and $|1\rangle\equiv\binom{1}{0}$, $|2\rangle\equiv\binom{0}{1}$.

Now assume that at time $t=t_0$ the atom, given initially by $|\psi_{\rm I}(t_0)\rangle=|1\rangle$, interacts with the first field for a time $\tau=l/v$, evolves freely for a time $T=L/v$, and finally interacts with the second field for another time τ. Thus, the final internal state is

$$|\psi_{\rm I}(t_0+2\tau+T)\rangle=U_{\rm I}^{(2)}(t_0+2\tau+T,t_0+\tau+T)\times U_{\rm I}^{(1)}(t_0+\tau,t_0)\times|\psi(t_0)\rangle. \tag{8}$$

This yields for the probability of a transmitted excited state our general result

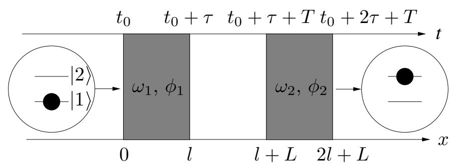

FIG. 1. Scheme of the Ramsey atom interferometer. The lower axis displays the position of the field edges, whereas the upper axis gives the corresponding instants of time for the classical trajectory of the moving atom.

$$
\begin{aligned}
P_{12}(\Delta_1,\Delta_2) &= |\langle 2|\psi_1(t_0+2\tau+T)\rangle|^2 \\
&= \Bigg| \sin\left(\frac{\Omega_2'\tau}{2}\right)\left[\cos\left(\frac{\Omega_1'\tau}{2}\right) - \frac{i\Delta_1}{\Omega_1'}\sin\left(\frac{\Omega_1'\tau}{2}\right)\right] \\
&\quad \times \frac{\Omega}{\Omega_2'} + e^{-i(\Delta_1-\Delta_2)(t_0+\tau)}e^{i\Delta_2 T}e^{i\phi}\sin\left(\frac{\Omega_1'\tau}{2}\right) \\
&\quad \times \left[\cos\left(\frac{\Omega_2'\tau}{2}\right) + \frac{i\Delta_2}{\Omega_2'}\sin\left(\frac{\Omega_2'\tau}{2}\right)\right]\frac{\Omega}{\Omega_1'}\Bigg|^2, \qquad (9)
\end{aligned}
$$

where $\phi=\phi_2-\phi_1$ is the phase difference between the two fields at $t=0$ (termed simply the "phase" hereafter). Note that $P_{12}(\Delta_1,\Delta_2)$ is periodic in the entrance time t_0 with period $2\pi/|\Delta_1-\Delta_2|$.

As a check we consider the limit of equal detuning, $\Delta_1=\Delta_2\equiv\delta$, $\Omega'=(\Omega^2+\delta^2)^{1/2}$, leading to

$$
\begin{aligned}
P_{12}(\delta,\delta) &= \frac{4\Omega^2}{\Omega'^2}\sin^2\left(\frac{\Omega'\tau}{2}\right)\left[\cos\left(\frac{\Omega'\tau}{2}\right)\cos\left(\frac{\delta T+\phi}{2}\right)\right. \\
&\quad \left. - \frac{\delta}{\Omega'}\sin\left(\frac{\Omega'\tau}{2}\right)\sin\left(\frac{\delta T+\phi}{2}\right)\right]^2, \qquad (10)
\end{aligned}
$$

which is independent of t_0 and coincides with the well-known result obtained by Ramsey [1].

For the sake of accuracy of the measurement it is important to study possible effects related to an imperfect control of t_0 and ϕ. First of all, the phase ϕ may show fluctuations. Therefore we also consider the phase-averaged expression

$$
\langle P_{12}(\Delta_1,\Delta_2)\rangle_\phi = \int_{-\pi}^{\pi} d\phi\, g(\phi) P_{12}(\Delta_1,\Delta_2), \qquad (11)
$$

where $g(\phi)$ is the distribution of ϕ. For a random, homogeneously distributed phase over the interval $[-w_\phi,w_\phi]$, one has $g(\phi)=(2w_\phi)^{-1}$ for $\phi\in[-w_\phi,w_\phi]$ and zero otherwise. Then the integration can be performed analytically and it leads to a factor of $\sin(w_\phi)/w_\phi$ which multiplies the cross terms of Eq. (9). For $w_\phi=0$ one recovers Eq. (9) with $\phi=0$, but for larger values of w_ϕ the cross terms are damped and the visibility of the interference pattern decreases.

In addition to phase fluctuations, one deals in general with an initial momentum and position distribution of the incoming atoms, such that t_0 is not completely fixed by the distance between the source and the first field and becomes a random variable with a distribution. Its influence on the interference pattern is studied in Sec. VI.

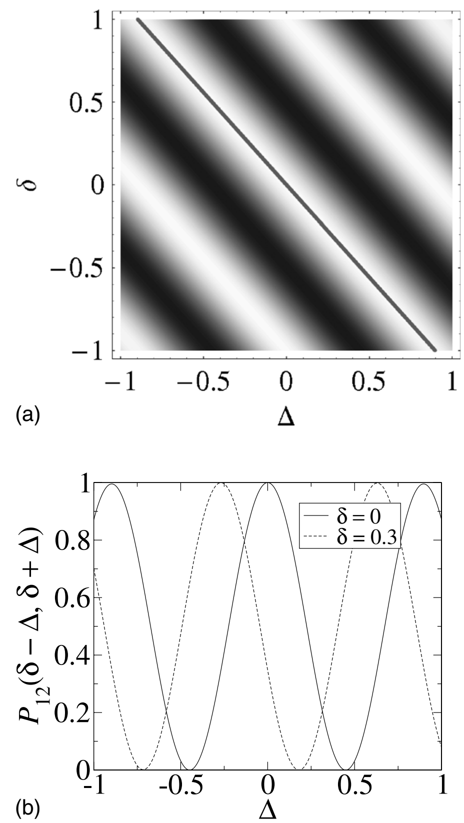

FIG. 2. (a) Contour plot of $P_{12}(\delta-\Delta,\delta+\Delta)$ for $w_\phi=0$, $t_0=0$, $\tau=1$, $T=5$, $\Omega=\pi/(2\tau)$. White color corresponds to a value of 1 whereas black corresponds to 0. The straight gray line visualizes the slope S of the pattern, given by Eq. (12). (b) Two cuts of for $\delta=0$ and 0.3. For all plots we use dimensionless units with $\hbar=m=1$.

IV. AVERAGE AND RELATIVE DETUNING

Let us assume that the two oscillator frequencies are $\omega_{1,2}=\omega\pm\Delta$. We call $\delta=\omega-\omega_{21}=(\Delta_1+\Delta_2)/2$ the *average detuning* and $\Delta=(\Delta_2-\Delta_1)/2$ the *relative detuning*. The additional parameters Δ and t_0 lead to new effects in the interference pattern that may be used to adjust ω to the nominal atomic frequency ω_{21}, i.e., to find the point $\delta=0$. The plot of $P_{12}(\delta-\Delta,\delta+\Delta)$ as a function of δ and Δ for fixed values of t_0 and for $w_\phi=0$ shows a regular pattern of maxima and minima [Figs. 2(a) and 3(a)]. A cut in the $\Delta=0$ plane would give back the usual Ramsey pattern $P_{12}(\delta,\delta)$ [see Eq. (10)] but for any other value of Δ the fringes are shifted. An interesting feature is that for increasing values of the entrance time t_0 the fringe pattern becomes tilted and narrower with respect to Δ. The slope S of the lines of maxima of the pattern can be determined from the condition $\partial_\Delta P_{12}(\delta-\Delta,\delta+\Delta)=0$. Solving this equation in first order of Δ and δ yields for the slope, with $\phi=0$,

$$
\begin{aligned}
S &= \{4\Omega\tau[\cot(\Omega\tau/2)-\sin(\Omega\tau)] - 8\cos(\Omega\tau) - [T+2(t_0 \\
&\quad +\tau)]^2\Omega^2[1+\cos(\Omega\tau)]\}\{\Omega[T+2(t_0+\tau)]\times[\Omega T \\
&\quad +\Omega T\cos(\Omega\tau)+2\sin(\Omega\tau)]\}^{-1}. \qquad (12)
\end{aligned}
$$

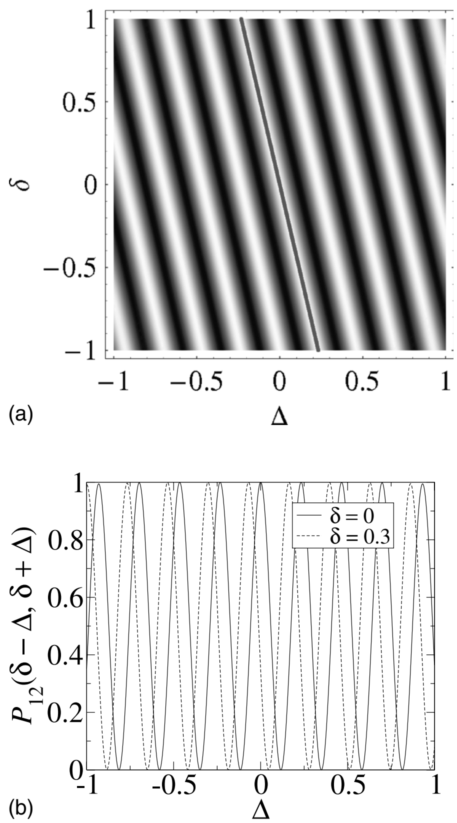

FIG. 3. (a) As in Fig. 2(a), but for $t_0=10$. (b) Two cuts of (a) for $\delta=0$ and $\delta=0.3$.

This expression reproduces the actual slope perfectly as can be seen from Figs. 2(a) and 3(a).

A plot of $P_{12}(\delta-\Delta,\delta+\Delta)$ as a function of the relative detuning Δ and for fixed average detuning δ is shown in Figs. 2(b) and 3(b) for two different values of t_0 and for $w_\phi=0$. This pattern becomes centered at $\Delta=0$ if $\delta=0$. Thus, by observing the central peak shift from $\Delta=0$, given by δ/S, one may decide whether the average detuning δ is zero or not. By increasing t_0 the fringes with respect to Δ become narrower and the determination of the shift is easy even for a poor resolution of P_{12}.

Next, we study the effect of $w_\phi>0$, i.e., of a random and homogeneously distributed phase between $-w_\phi$ and w_ϕ. It can be seen from Fig. 4 that this leads to the above mentioned reduction of the visibility of the fringes. The position of their maxima as well as their widths remain the same. For $w_\phi=\pi$, corresponding to a totally homogeneous phase distribution, the pattern would be completely suppressed, but we emphasize that quite large phase uncertainties (e.g., $w_\phi=1.0$) still lead to excellent visibility of the pattern.

V. THE SYMMETRICAL DETUNING CASE

To understand better the role of t_0, we shall restrict this section to the resonance condition $\delta=0$. The only difference from the general case $\delta\neq0$ is a shift of the pattern as has been discussed above. We shall also assume $w_\phi=0$ within this section. According to Eq. (9) one finds

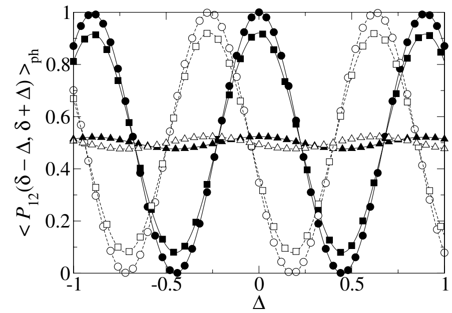

FIG. 4. Phase-averaged interference pattern $\langle P_{12}(\delta-\Delta,\delta+\Delta)\rangle_{ph}$ given by Eq. (11) for $t_0=0$, $\tau=1$, $T=5$, $\Omega=\pi/(2\tau)$. Solid lines and full symbols correspond to $\delta=0$, dashed lines and open symbols correspond to $\delta=0.3$. Parameters of the phase distribution are $w_\phi=0$ (circles), 1.0 (squares), and 3.0 (triangles).

$$P_{12}(-\Delta,\Delta)=\frac{4\Omega^2}{\Omega'^2}\sin^2\left(\frac{\Omega'\tau}{2}\right)\cos^2[\Delta(t_0+\tau+T/2)]\times\left[\cos^2\left(\frac{\Omega'\tau}{2}\right)+\frac{\Delta^2}{\Omega'^2}\sin^2\left(\frac{\Omega'\tau}{2}\right)\right]. \quad (13)$$

We plot $P_{12}(-\Delta,\Delta)$ in Fig. 5(a) as a function of Δ and t_0. The interference pattern with respect to Δ becomes narrower if the initial entrance time t_0 is increased. This may appear astonishing at first sight since we expect periodicity in t_0. As is shown in Fig. 5(b), P_{12} is indeed periodic in t_0 for fixed relative detuning Δ, but with a detuning-dependent period $\pi/|\Delta|$, leading for increasing t_0 to a narrower pattern as a function of Δ. An estimate for the width of the central fringe is obtained if one expands $P_{12}(-\Delta,\Delta)$ in a series around $\Delta=0$. Assuming a $\pi/2$ pulse for the fields, $\Omega=\pi/(2\tau)$, this gives $P_{12}(-\Delta,\Delta)=1-[T+2(t_0+\tau)]^2\Delta^2/4+O(\Delta^3)$, such that the first zeros of the pattern are approximately given by

$$\Delta_0^{\pm}\simeq\pm\frac{2}{T+2(t_0+\tau)}. \quad (14)$$

The central width is inversely proportional to the sum of the intermediate crossing time T and the entrance time t_0. Basically, the narrowing is an effect of relative phase differences between the fields. Note the roles of t_0 and T in Eq. (14): first of all, t_0 is twice as efficient as T to produce a desired width; moreover t_0 is the time for free flight of ground-state atoms, whereas T is a free-flight time for atoms with excited components, which are amenable to decay.

VI. ATOMIC CLOUDS

Up to now, the monochromatic case with a fixed entrance time t_0 has been considered. In general, for an incoming cloud of atoms, the entrance and crossing times for the individual atoms will be different, and one has to integrate P_{12} over all possible classical trajectories, weighted by a phase space distribution $W(x,k)$. We assume here that $W(x,k;t)$ describes a minimum uncertainty packet when its center impinges the origin $x=0$ at time $t=t_0^c$,

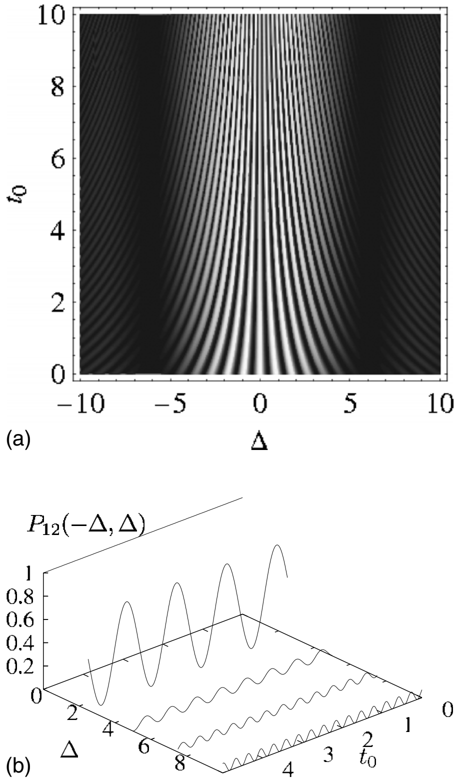

FIG. 5. (a) Contour plot of $P_{12}(-\Delta,\Delta)$ as a function of Δ and t_0 for $w_\phi=0$, $\tau=1$, $T=5$. With increasing t_0, the interference pattern with respect to Δ becomes narrower. The zeros of $P_{12}(-\Delta,\Delta)$ at $\Delta\approx\pm 6$ are independent of t_0 and they are given by $\sin(\Omega'\tau/2)=0$ according to Eq. (13). (b) $P_{12}(-\Delta,\Delta)$ as a function of t_0 for $\Delta=\{0,2.5,5,7.5,10\}$. P_{12} is periodic in t_0 with a period that depends on Δ. We emphasize the fact that $P_{12}(0,0)=1$ independent of t_0 (straight line), indicating that the central peak remains stable irrespective of the entrance time.

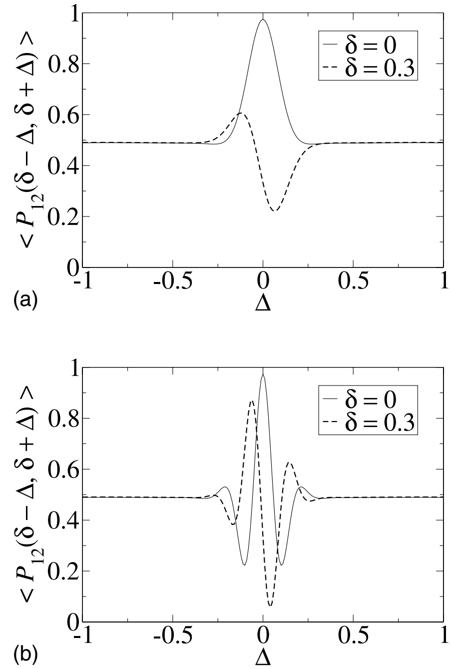

FIG. 6. $\langle P_{12}(\delta-\Delta,\delta+\Delta)\rangle$ as a function of Δ for $t_0^c=$(a) 0 and (b) 10. Other parameters are $w_\phi=0$, $l=1$, $L=5$, $k_c=1$, $\delta k=0.1$, $\delta x=5$. The Rabi frequency has been chosen as a $\pi/2$ pulse for the mean velocity, $\Omega=\pi\hbar k_c/(2ml)$.

$$W(x,k;t)=\frac{1}{2\pi\delta_x\delta_k}\exp\left(-\frac{(k-k_c)^2}{2(\delta_k)^2}\right)\times\exp\left(-\frac{[x-\hbar k(t-t_0^c)/m]^2}{2(\delta_x)^2}\right), \qquad (15)$$

where δ_x and $\hbar\delta_k$ are the uncertainties of position and momentum, connected by $\delta_x\delta_k=1/2$, and $\hbar k_c$ is the mean momentum.

Now, in Eq. (9) one has to replace τ by $l/v=ml/\hbar k$, T by $L/v=mL/\hbar k$, and t_0 by a varying entrance time, given by $t_0^c-x/v=t_0^c-mx/\hbar k$ when x and $\hbar k$ are positions and momenta at t_0^c. Thus, the excitation probability becomes

$$\langle P_{12}(\delta-\Delta,\delta+\Delta)\rangle=\int_{-\infty}^{\infty}dx\,dk\,W(x,k;t_0^c)P_{12}(\delta-\Delta,\delta+\Delta). \qquad (16)$$

In this equation, the x integration can be performed analytically whereas the k integration has to be performed numerically and the result is shown in Fig. 6 as a function of Δ for fixed values of δ and t_0^c. For large Δ the outer fringes are averaged out, but the central fringes survive and they exhibit a shift for $\delta\neq 0$. The width of these fringes can be controlled by t_0^c, as in the monochromatic case. Other phase-space distributions may of course be found in practice, but the important point is that P_{12} for $\delta=0$ in Eq. (13), is symmetrical around $\Delta=0$ for any t_0, so that the averaging will not induce undesired frequency shifts.

VII. PHASE-RELATED SYSTEMATIC SHIFTS

The narrowing that may be achieved in the interference pattern of $P_{12}(\delta-\Delta,\delta+\Delta)$ by sweeping over Δ for each δ, instead of sweeping over δ for $\Delta=0$ as in the usual Ramsey method, is quite evident in Fig. 3(a) (compare the horizontal and vertical cuts). The narrow Δ pattern may be used in practice to steer the unknown δ until the central peak is found at $\Delta=0$. For $\phi=0$ or for a symmetrical phase average around $\phi=0$, this corresponds to the resonance condition $\delta=0$ and serves to identify the atomic frequency. There are, however, different physical effects that shift the central peak and have to be taken into account. For a practical use of the proposed two-frequency method, the systematic shifts, or "frequency offsets," should not be worse than the ones which already affect the standard (one-frequency) Ramsey method.

With the help of Eq. (9) we may in particular study systematic effects in which ϕ is not zero or the average of the distribution of phases is nonzero. In the standard Ramsey setup this is typically due to the unequal lengths of the arms of the microwave cavity, and the corresponding offset scales as $\delta_0=-\phi/T$ for $\tau\ll T$ (which is assumed to hold hereafter), where δ_0 is the value of δ for the central maximum,

$$\left.\frac{\partial P_{12}(\delta,\delta)}{\partial \delta}\right|_{\delta=\delta_0} = 0.$$

This scaling can be found by expanding Eq. (10) around $\delta=0$. We may immediately check from the general expression (9) that the value of δ that satisfies

$$\left.\frac{\partial P_{12}(\delta-\Delta,\delta+\Delta)}{\partial \Delta}\right|_{\delta=\delta_0',\Delta=0} = 0$$

at $\Delta=0$, which we call δ_0', is also shifted by the same amount for $\pi/2$ pulses. If the pulses deviate slightly from the $\pi/2$ case, say $\Omega=\pi/(2\tau)+\epsilon$, the dominant offset is still the same in both methods (standard Ramsey and two-frequency), namely, $-\phi/T$, except for a higher-order difference $\delta_0-\delta_0'$ proportional to $\phi\epsilon\tau^3/T^3$. In other words, the two-frequency method does not aggravate the systematic shift. We have also performed averages over ϕ similar to the ones in Secs. III and IV, but for displaced phase distributions, not centered at $\phi=0$. Figures, not displayed, entirely analogous to Figs. 3 and 4, are observed, affected by the mentioned frequency offset and, as with centered phase distributions, by a smaller visibility.

Other systematic dependences might occur: we have also examined the consequences of a linear relation or chirp between ϕ and Δ, $\phi=\phi_0+b\Delta$. The results, however, are the same as before, with ϕ_0 playing the role of ϕ in the expression for the frequency offset, and b being added to $2t_0$ without altering the value of δ_0 or δ_0' at the central peak in any of the two methods.

VIII. DISCUSSION

In this paper we have studied the interference fringes in a Ramsey interferometer where the separated fields have different detuning. The excitation probability $P_{12}(\Delta_1,\Delta_2)$, derived within a semiclassical picture neglecting quantum reflections at the fields depends on the entrance time t_0 of the atom at the first field, and, in addition, on the initial phase difference ϕ of the two fields. Our main result is that the interference pattern for $\phi=0$ as a function of the relative detuning $\Delta=(\Delta_2-\Delta_1)/2$ exhibits a shift of the central maximum if the average detuning δ differs from zero. This shift has been quantified and it may be used to steer an oscillator toward the atomic frequency. The advantage of this approach is that the width of the interference fringes versus Δ can be made very small because it is shown to be inversely proportional to the entrance time t_0.

Additionally, we have studied the effect of possible fluctuations or systematic shifts in the relative phase between the two fields. Assuming a distribution with some width w_ϕ around $\phi=0$, we have shown that all the described features of the interference pattern remain unchanged and only the visibility of the fringes decreases for increasing w_ϕ. A displaced phase distribution leads to a frequency offset which does not aggravate the one already present in the ordinary, one-frequency, Ramsey method. Moreover, we have demonstrated the stability of the central fringes for a distribution of velocities and thus of entrance times t_0, as in the standard Ramsey experiment.

The analysis of the experimental design and implementation of the proposed double-frequency interferometry is beyond the scope of this paper, where we have investigated and predicted from a theoretical perspective the main consequences that can be extracted from the general probability formula (9) and several fluctuations and averaging effects that may be expected. The specific experimental setting for phase, velocity, and frequency field control would determine their importance, but the preliminary results indicate a remarkable stability of the positive features of the approach.

In spite of our focus on moving atoms and fields in separate regions, we note that the same effects arise for trapped atoms and time-varying fields. Here, the Rabi frequency in Eq. (4) has to be replaced by a time-dependent version, but the general result in Eq. (9) would still hold. Also, it is natural to set for all trapped atoms $t_0=0$, corresponding to the switching on of the Ramsey fields, but the narrowing effect of the free-flight time parameter t_0 may be achieved by a chirp of the form $\phi=b\Delta$ as discussed in the previous section. For trapped atoms, turning on and off the fields may lead to transients and deviations from the mesa-shaped fields.[3] For simplicity, we presented only the case of mesa-shaped fields, but we have performed numerical studies for more realistic field shapes, used also for Stimulated Rapid Adiabatic Passage (STIRAP) calculations [13], and they show similar results [14].

As an outlook, it would be worthwhile to investigate the Ramsey fringes for differently detuned fields beyond the semiclassical approximation, i.e., taking into account quantum reflections at the fields for very slow (ultracold) atoms. This has been shown to yield interesting effects with a single frequency [10].

ACKNOWLEDGMENTS

The authors thank Guery-Odelin and M. G. Raizen for helpful discussion. This work has been supported by Ministerio de Educación y Ciencia (FIS2006-10268-C03-01) and UPV-EHU (00039.310-15968/2004). D.S. acknowledges support from the German Academic Exchange Service (DAAD).

[3]For moving atoms the temporal transients can be avoided by sending atomic pulses when a stationary field intensity has been settled.

[1] N. F. Ramsey, Phys. Rev. **78**, 695 (1950); *Molecular Beams* (Clarendon Press, Oxford, 1956).
[2] D. B. Sullivan *et al.*, J. Res. Natl. Inst. Stand. Technol. **106**, 47 (2001); S. Bize *et al.*, J. Phys. B **38**, S449 (2005); J. Vanier and C. Audoin, Metrologia **42**, S31 (2005).
[3] R. Wynands and S. Weyer, Metrologia **42**, S64 (2005).
[4] P. Laurent *et al.*, Eur. Phys. J. D **3**, 201 (1998); Ch. Salomon *et al.*, C. R. Acad. Sci., Ser IV: Phys., Astrophys. **2**, 1313 (2001).
[5] A. Peters *et al.*, Philos. Trans. R. Soc. London, Ser. A **355**, 2223 (1997).
[6] J. C. Bergquist, W. M. Itano, and D. J. Wineland, Phys. Rev. A **36**, 428 (1987).
[7] T. Ido and H. Katori, Phys. Rev. Lett. **91**, 053001 (2003).
[8] C. J. Bordé, C. R. Acad. Sci., Ser IV: Phys., Astrophys. **2**, 509 (2001); P. Wolf *et al.*, in *Proceedings of the Sixth Symposium on Frequency Standards and Metrology*, edited by P. Gill (World Scientific, Singapore, 2002) p. 593; C. J. Bordé, Metrologia **39**, 435 (2002).
[9] *Atom Interferometry*, edited by P. R. Berman (Academic Press, San Diego, 1997).
[10] D. Seidel and J. G. Muga, Eur. Phys. J. D **41**, 71 (2007).
[11] I. Lizuain, J. G. Muga, and A. Ruschhaupt, Phys. Rev. A **74**, 053608 (2006).
[12] J. A. Damborenea, I. L. Egusquiza, G. C. Hegerfeldt, and J. G. Muga, J. Phys. B **36**, 2657 (2003).
[13] M. P. Fewell, B. W. Shore, and K. Bergmann, Aust. J. Phys. **50**, 281 (1997).
[14] D. Seidel and J. G. Muga, available at: quant-ph/0606073.
[15] E. Riis and A. G. Sinclair, J. Phys. B **37**, 4719 (2004).